PROGRESS IN COLOR, COLORANTS AND COATINGS

available online @ www.pccc.icrc.ac.ir

Prog. Color Colorants Coat. 8(2015), 69-86

Ministry of Science, Research and Technology
Institute for Color Science and Technology

Application of Electrochemical Noise to Investigate Corrosion Inhibition Properties of Some Azole Compounds on Aluminum in 0.25 M HCl

B. Ramezanzadeh[*1], M. Mehdipour[2], S. Y. Arman[3]

[1.] Assistant Professor, Department of Surface Coatings and Corrosion, Institute for Color Science and Technology, P. O. Box: 16765-654, Tehran, Iran

[2.] MSc student, Department of minning and Material Engineering, Amirkabir University of Technology, P.O. Box 15875-4413, Tehran, Iran.

[3.] MSc student, Department of minning and Material Engineering, Amirkabir University of Technology, P.O. Box 15875-4413, Tehran, Iran.

ARTICLE INFO

Article history:
Received: 14-10-2014
Final Revised: 22-11-2014
Accepted: 06-12-2014
Available online: 06-12-2014

Keywords:
Aluminum
Corrosion inhibitors
electrochemical impedance spectroscopy
electrochemical noise resistance

ABSTRACT

The corrosion inhibition properties of the benzothiazole and benzotriazole inhibitors on the aluminum in 0.25 M HCl solution were studied. Electrochemical impedance spectroscopy, electrochemical noise and potentiodynamic polarization techniques were used to investigate inhibition properties of the inhibitors. Scanning electron microscope was also utilized in order to investigate the surface morphology of the samples. Results showed that benzotriazole and benzothiazole significantly reduced the corrosion rate of the aluminum. A higher corrosion inhibition efficiency of the benzotriazole compared with benzothiazole was obtained. It was shown that electrohemical noise is an appropriate technique for studying the corrosion inhibition properties of the corrosion inhibitors. Prog. Color Colorants Coat. 8(2015), 69-86 © Institute for Color Science and Technology.

1. Introduction

Aluminum as the most consuming non-ferrous metal with excellent properties like lightness, thermal and electrical conductivity has usage in wide range of applications from home appliances to aerospace industry [1-4]. The amazingly fast reaction of aluminum with its overwhelming atmosphere and formation of a passive layer on the surface could protect the aluminum from corrosion and further destruction. But this layer cannot be formed in highly corrosive media like acidic solutions which could limit the application of the aluminum for some industries [5-7]. Although the corrosion cannot be completely prevented, there are approaches to slow down the process; cathodic and anodic protection, organic and inorganic coatings, and corrosion inhibitors are the most famous ones. Among all these methods, the corrosion inhibitors especially organic inhibitors are popular choices for many applications and

*Corresponding author: ramezanzadeh-bh@icrc.ac.ir

environments [8-17]. For a long time, scientists tried to characterize the interaction among metal, inhibitor and solution which lead to corrosion inhibition by organic inhibitors. Most of them concluded that adsorption of the organic inhibitor molecules instead of water molecules on the surface of metals and formation of a protective layer is the dominant mechanism. Existences of π bonds or hetero-atoms (e.g. O, N, S, and P) in the chemical structure of the organic inhibitors are believed to be responsible for their inhibition properties. It has been found that most of the corrosion inhibitors are heavily toxic and environmentally hazardous materials. However, they have been widely used due to their high corrosion inhibition properties [18-24]. In the matter of aluminum and organic inhibitors, Safak et al. [25] studied the corrosion inhibition properties of some Schiff based corrosion inhibitors on the aluminum in HCl solution. They found that the Schiff based corrosion inhibitors could reduce the corrosion of aluminum significantly. Fares et al. [26] studied the inhibition properties of the Pectin as a green inhibitor on the aluminum in HCl solution. A corrosion inhibition efficiency of 91% was obtained in the presence of Pectin on the aluminum in HCl solution.

The adsorption of azole derivatives on the iron, copper and aluminum surface has been studied by Kovacevic and Kokalj [27] by density functional theory (DFT). They showed that the role of metal d-states on the molecule surface bonding would be really important for the reactive transition metals with open d-band. The azole derivatives can be adsorbed on the Fe surface either parallel (through pronounced π-d hybridization) or vertical (through sigma bond) to the surface. The high density of "d" state around the Fermi level of the energy could be responsible for this matter. However, unlike Fe, aluminum does not have open d-band for reaction with inhibitors through π-d hybridization. The density of states (DOS) for the aluminum in the vicinity of Fermi energy consists of a very broad and flat sp-band. Due to the lower energy of "sp" band compared to "d" state in the vicinity of Fermi energy, the chemical adsorption of the inhibitors on the aluminum surface is lower than the iron. In fact, benzotriazole (BT) and benzothiazole (BTH) have large dipole moments which could interact with the metal surface by forming electrostatic dipole interactions. Naderi et al. [28] investigated the corrosion inhibition of BT and BTH on the stainless steel in acidic media. They found that BTH showed higher inhibition efficiency that BT in 1 M HCl solution on the stainless steel.

To the best of our knowledge, there is no systematic work on studying the inhibitory effects of the BT and BTH on the aluminium in HCl solution. BT has acidic hydrogen (s) and unsaturated heteroatoms (N). However, BTH has two unsaturated heteroatoms of N and S. Therefore, they can be presented in different forms of neutral, deprotonated and protonated. Depending on the form of the inhibitors, the inhibitors molecules may orient on the aluminium surface in different manners. In this study, we will investigate the differences between the inhibition action of these two azole derivatives.

Electrochemical impedance spectroscopy (EIS) and linear polarization are two well-known methods for the corrosion studies [29]. Electrochemical noise (EN) as a novel technique with numerous advantages has drawn a lot of attention in the past few years and many researchers have tried to utilize this method for different applications. EN occurs naturally in the metal/solution interface due to all procedures involved in corrosion phenomena (migration of electroactive particles, cathodic and anodic reactions, pitting initiation, etc) and the fluctuations in the potential and current generated spontaneously by the process is recorded. Since in this method there is no need to apply external perturbation, it can be completely distinctive from conventional linear polarization and EIS methods [29, 30].

Through the beneficial application of the electrochemical noise measurements we aim to compare the inhibition properties of these two well-known organic inhibitors on the aluminum in 0.25M HCl solution. Furthermore, this paper tries to compare the results obtained from various electrochemical techniques.

2. Experimental

2.1. Material and sample preparation

The corrosion inhibition properties of the BT and BTH were studied on an aluminum alloy in 0.25 M HCl solution. To this end, an aluminum alloy with chemical composition given in Table 1 was utilized. The surface of the aluminum specimens was grinded by emery papers with grit size 80 to 1200.

Table 1: Chemical composition of the aluminum specimen obtained from SEM/EDS analysis.

Al	Si	Fe	Cu	Mn	Mg	Cr
98.25	0.38	0.62	0.05	0.54	0.15	0.01

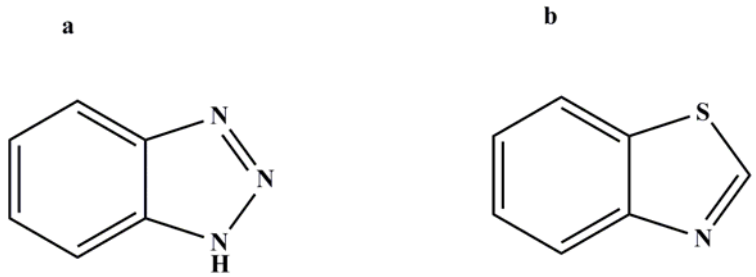

Figure 1. Chemical structures of a) Benzotriazole (BT) and b) Benzothiazole (BTH).

The grinded samples were then rinsed in distilled water and dried in air, followed by degreasing with acetone. It has been aimed to compare the corrosion inhibition properties of BTH (C_7H_5NS) and BT ($C_6H_5N_3$) on the aluminum surface in 0.25 M HCl solution at different concentrations. The inhibitors were used in a wide range of concentrations (25 to 1000 ppm). The chemical structures of the inhibitors are shown in Figure 1. The corrosion inhibitors and HCl solution were supplied from Merck (Germany).

2.2. Techniques

2.2.1. Scanning electron microscope (SEM)

SEM was used in order to investigate the surface morphology of the samples before and after exposure to HCl solution in the presence and absence of corrosion inhibitors. The test was carried out by a Philips model SEM at different magnifications.

2.2.2. Potentiodynamic DC polarization

The corrosion inhibition properties of the aluminum in HCl solution in the presence and absence of inhibitors were studied by a DC polarization technique. The test was carried out in an electrochemical cell including aluminum specimen (working electrode), platinum plate (counter electrode) and saturated calomel (reference) electrode. The polarization plots were obtained at sweep rate of 1 mV/s in the range of ±200 mV from the open circuit potential (OCP). The OCP was measured after 1 h (after reaching to steady state). The test was carried out on 1 cm^2 of the samples in 0.25 M HCl solution in the presence and absence of BT and BTH. The electrochemical parameters including corrosion current density (I_{corr}), corrosion inhibition efficiency (η) and corrosion rate were obtained from the polarization curves. The corrosion current density (I_{corr}) was obtained using Tafel extrapolation technique and general purpose electrochemical software (GPES).

2.2.3. EIS and EN measurements

Electrochemical impedance spectroscopy (EIS) and electrochemical noise analysis (EN) were utilized to investigate the corrosion inhibition properties of the inhibitors in 0.25 M HCl solution on the aluminum surface. The measurements in EIS test were carried out by an AUTOLAB G1 at perturbation and frequency range of 10 mV and 10 kHz to 10 mHz, respectively. To this end, an electrochemical system including platinum plate (auxiliary electrode), saturated Calomel electrode (reference) and aluminum sheet (working electrode) was used. For the EN analysis, the electrochemical potential and current noise were measured simultaneously by connecting two aluminum panels and Calomel reference electrode to the EN port of the Autolab PGSTAT12. The measurements were made during a period of 1000 s at 1-s intervals (frequency range from 1 mHz to 0.5 Hz). Data were determined by the expressions $f_{max} = 1/2\ \Delta t$ and $f_{min} = 1/N\ \Delta t$ where Δt and N are the sample interval and the total number of data recorded, respectively. The DC trend was removed from the measured data before statistical data analysis through moving average removal (MAR) method [27].

Both EIS and EN measurements were carried out on 1 cm^2 of the aluminum in 0.25 M HCl solution in the presence and absence of BT and BTH inhibitors. In both EIS and EN techniques, the test was carried out using three replicates to ensure the measurement repeatability.

3. Results and discussion

3.1 DC polarization measurements

The corrosion inhibition properties of the aluminum in 0.25 M HCl solution in the presence and absence of BT and BTH were studied by DC polarization measurements. Variation of potential versus current density of different samples is shown in Figure 2.

Electrochemical parameters including corrosion current density (I_{corr}), corrosion potential (E_{corr}) and Tafel slopes (β_a and β_c) were obtained from the polarization curves (Figure 2). The results are shown in Table 2.

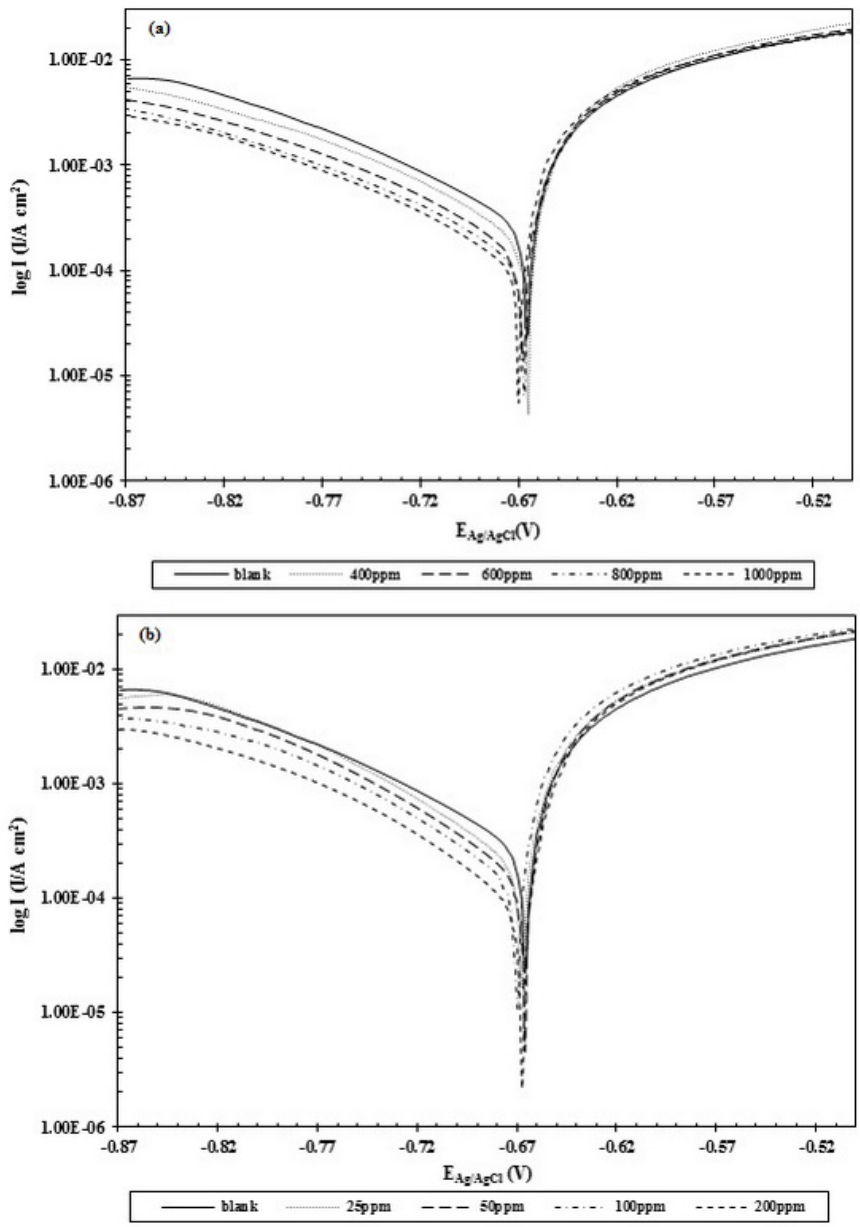

Figure 2. Current versus potential of the Al samples exposed to 0.25 M HCl in the presence of (a) BTH and (b) BT inhibitors at different concentrations.

Table 2: Electrochemical parameters obtained from polarization measurements for the Al samples exposed to BT and BTH at different concentrations in 0.25 M HCl solution.

Sample	β_a(mV/decade)	β_c(mV/decade)	E_{corr} (mV)	I_{corr} (μA cm^{-2})	corrosion rate (mpy)	R_p (Ω cm^2)	Efficiency (%)
0 ppm	125	22.9	-665	325	3.0	25	--
BT-25 ppm	97	17.2	-664	211	2.5	30	35
BT-50 ppm	95	13.4	-663	166	1.9	35	49
BT-100 ppm	97	13.4	-669	149	1.7	34	54
BT-200 ppm	92	14.4	-664	95	1.1	56	70
BTH-400 ppm	112	17.7	-663	219	2.5	30	32
BTH-600 ppm	112	19.1	-667	174	2.0	40	46
BTH-800 ppm	119	19.3	-668	153	1.7	47	52
BTH-1000ppm	112	14.2	-668	125	1.4	50	61

Polarization resistance (R_p) values were calculated from equation (1):

$$R_p = (\beta_a \times \beta_c)/(2.3 \times I_{corr} (\beta_a + \beta_c)) \quad (1)$$

where R_p, β_a, β_c and I_{corr} show polarization resistance, anodic Tafel slope, cathodic Tafel slope and corrosion current density, respectively.

As can be seen in Table 2 and Figure 2, the I_{corr} and corrosion rate were reduced in the presence of both inhibitors. The R_p of the aluminum increased significantly when different concentrations of BT and BTH were added to HCl solution. The decrease in I_{corr} and the increase in R_p were more and more pronounced with increasing the inhibitor concentration. These observations reveal that the corrosion inhibitors could efficiently reduce the dissolution rate of aluminum in HCl solution. It can be clearly seen from the results shown in Table 2 that both anodic and cathodic Tafel slopes were reduced with increasing the inhibitors concentration. However, the decrease in anodic current density was not significant. The variations of β_c and β_a in Table 2 indicate the influence of inhibitors on the kinetics of hydrogen evolution and the inhibitor adsorption on the aluminium surface. Results show that the decrease in cathodic current density was higher than anodic one in the presence of both BTH and BT. This observation reveals that these inhibitors could reduce the dissolution rate of aluminum by reducing the cathodic reactions. These observations reveal that the adsorbed inhibitors molecules formed a protective film on the surface of the aluminum. The protective layer could reduce the aluminum dissolution rate significantly. Results showed the lower I_{corr} and higher R_p values of the aluminum sample exposed to the HCl solution containing BT compared with BTH. This can show the higher corrosion protection properties of the aluminum in the presence of BT.

3.2. Electrochemical impedance spectroscopy (EIS) measurements

The corrosion performance of the aluminum in HCl solution in the presence and absence of different concentrations of BT and BTH was also studied by an EIS technique. The Nyquist and Bode plots are shown in Figure 3.

Figure 3 shows that BTH and BT increase the corrosion resistance of the aluminum. The Nyquist plots consist of a capacitive loop at high frequencies and inductive loop at low frequencies. This can demonstrate the common behavior of the aluminum in HCl solution [31-35]. Using electrical circuit shown in Figure 4, the electrochemical parameters including charge transfer resistance (R_{ct}), polarization resistance (R_p), constant phase element (CPE), inductance resistance (R_L), inductor (L) and impedance at 1 Hz were obtained (Table 3). The representative example of using this equivalent circuit to fit the experimental data is shown in Figure 5. The chi-squared (χ^2) is used to evaluate the precision of the fitted data [31].

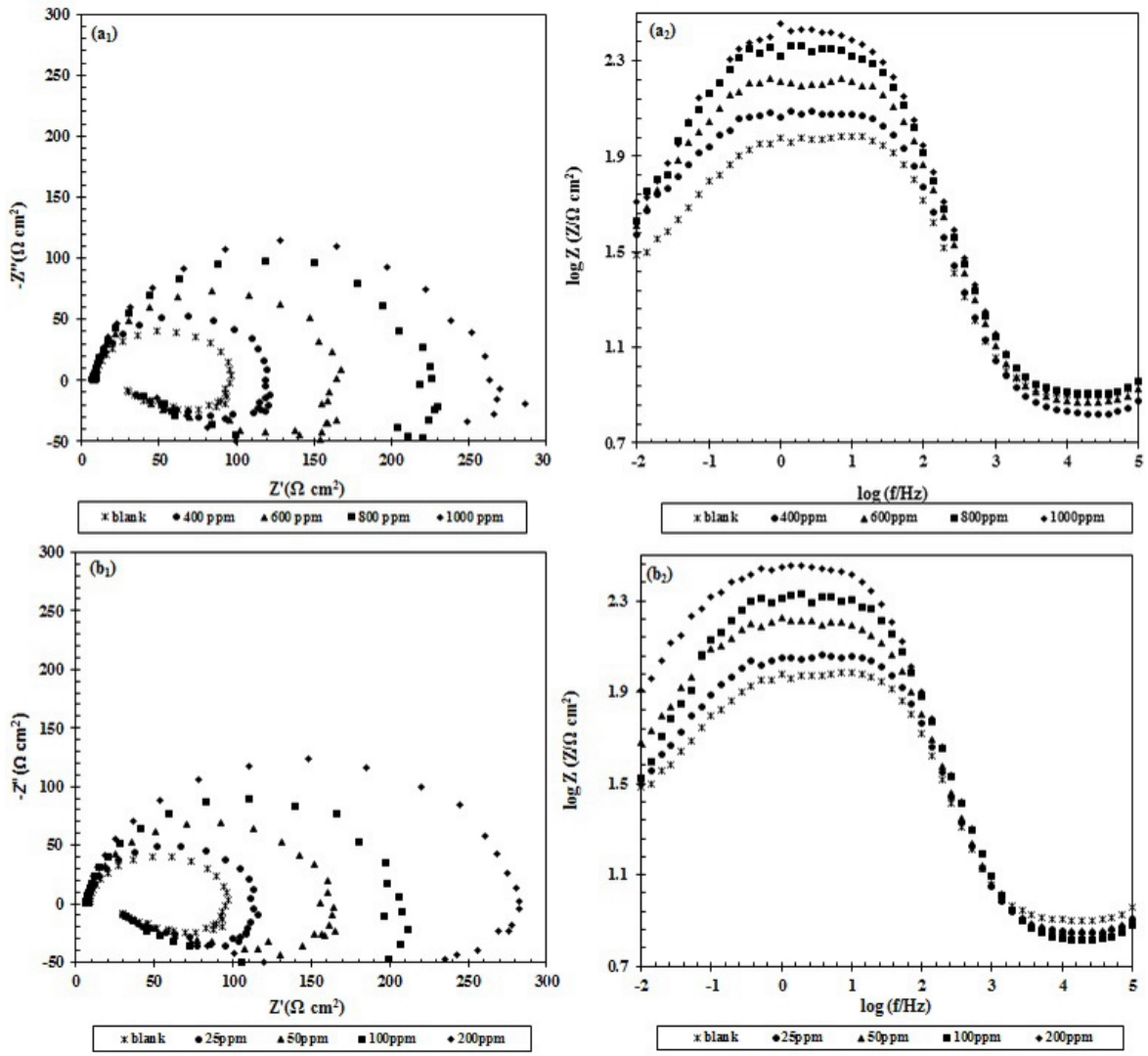

Figure 3. Nyquist and Bode plots of the samples exposed to 0.25 M HCl solution containing BTH (a_1 and a_2), and BT (b_1 and b_2) at different concentrations.

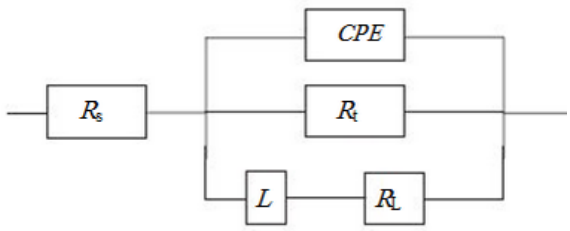

Figure 4. Electrical equivalent circuit used to analyze the results obtained from EIS (Figure 3).

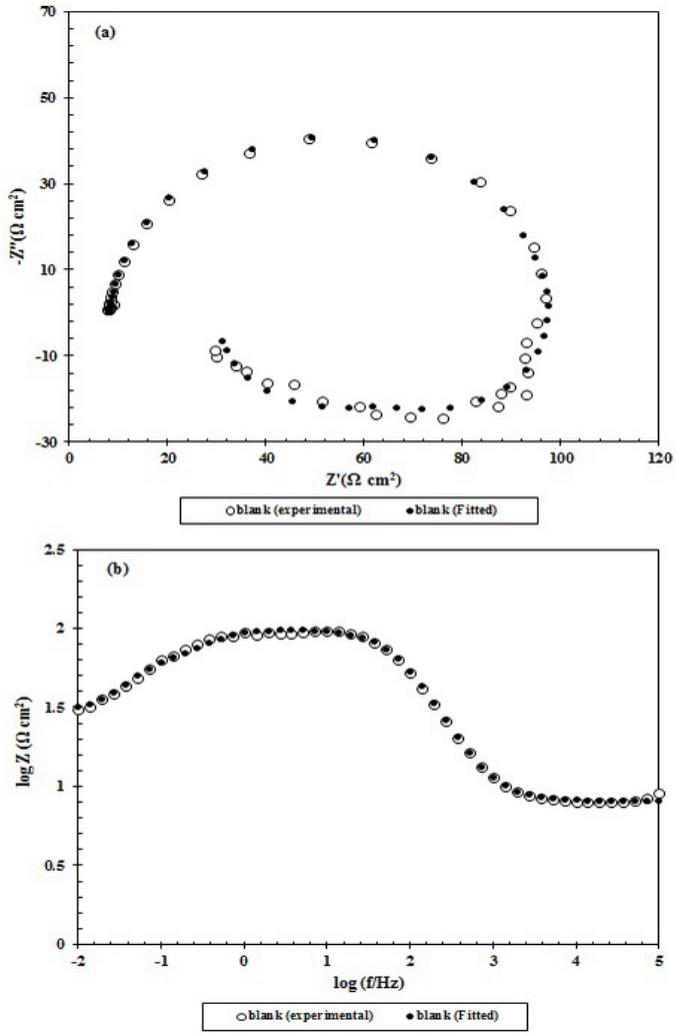

Figure 5. The representative figure of using the equivalent circuit to fit the experimental data for 0.25 M HCl without inhibitor, (a) Nyquist and (b) Bode plots.

Table 3: Electrochemical parameters obtained from EIS measurements for the Al samples exposed to BT and BTH at different concentrations in 0.25 M HCl solution.

Sample	R_{ct} (Ω cm^2)	*CPE*		L (H cm^2)	R_L (Ω cm^2)	C_{dl} (μF cm^{-2})	R_p (Ω cm^2)	χ^2
		Y_0 (Ω^{-1}cm^{-2})	n					
0 ppm	86	3.48×10^{-5}	0.95	143	38.08	26.44645	26.4	0.008
BT-25 ppm	106	3.23×10^{-5}	0.95	195	44	24.5	31.4	0.001
BT-50 ppm	152	3.35×10^{-5}	0.94	399	73	24.3	49.5	0.007
BT-100 ppm	207	3.27×10^{-5}	0.93	803	142	23.5	84.4	0.005
BT-200 ppm	264	2.79×10^{-5}	0.93	799	140	20.4	91.6	0.006
BTH-400 ppm	114	3.44×10^{-5}	0.94	301	62	24.3	40.4	0.008
BTH-600 ppm	155	2.52×10^{-5}	0.95	322	65	19.4	46.0	0.001
BTH-800 ppm	212	2.54×10^{-5}	0.94	373	73	19.1	54.6	0.008
BTH-1000ppm	248	2.41×10^{-5}	0.94	349	75	17.4	58.2	0.009

The low χ^2 shown in Table 3 indicates that the fitted data have good agreement with the experimental data.

Double layer capacitance (C_{dl}) and polarization resistance (R_p) values were calculated according to equations 2 and 3:

$$C_{dl} = Y_0 (2\pi f_{max})^{(n-1)} \quad (2)$$

$$R_P = (R_t - R_L)/(R_t + R_L) \times 100 \quad (3)$$

where C_{dl}, f_{max}, Y_0 and n represent double layer capacitance, frequency at which the imaginary component of the impedance is maximum, admittance constant and the empirical exponent, respectively. The passive film presented on the surface of the aluminum is not stable in HCl solution. As a result, the corrosion resistance of the aluminum in HCl solution is very low in the absence of the inhibitors. Results presented in Table 2 can clearly show the decrease in C_{dl} values and the increase in impedance and R_{ct} in the presence of both inhibitors. It can be seen that the decrease in C_{dl} and the increase in R_p were more pronounced at higher concentrations of both inhibitors. The decrease in C_{dl} in the presence of inhibitors can be attributed to the local dielectric constant reduction and/or the increase in double layer thickness. These observations demonstrate that the adsorption of inhibitors molecules on the surface of the aluminum significantly enhanced its corrosion resistance. The water molecules replacement with adsorbed inhibitor molecules on the metal surface resulted in protective film formation. The large BTH and BT molecules adsorption on the surface of aluminum led to the increase in double layer thickness and therefore the capacitance reduction. Results obtained from EIS analysis show the superior corrosion inhibition properties of BT compared with BTH. This observation reveals that BT molecules could form better protective film on the surface of the aluminum than BTH. The results obtained from EIS analysis are completely in agreement with the results obtained from polarization measurements.

3.3. Electrochemical noise (EN) measurements

Electrochemical noise was utilized in order to investigate the time records of the electrochemical current noise and the corresponding *PSD* (*I*) plots of the aluminum samples in 0.25 M HCl solutions in the presence and absence of the BT and BTH inhibitors. The results obtained are presented in Figures 6 and 7.

Figure 6 shows lower amplitude of current fluctuations generated in the presence of both inhibitors compared with the HCl solution without inhibitors. This observation reveals that the noise level reduced significantly in the presence of the inhibitors. This finding demonstrates that the inhibitors could reduce the corrosion of aluminum considerably. To calculate the noise resistance, the standard deviation from potential and current were calculated from equations 4 and 5, respectively.

$$\sigma_E = \sqrt{\sum_{i=1}^{n} (E_i - m_E)^2 / n} \quad m_E = \sum_{i=1}^{n} E_i / n \quad (4)$$

$$\sigma_i = \sqrt{\sum_{i=1}^{n} (I_i - m_i)^2 / n} \quad m_i = \sum_{i=1}^{n} I_i / n \quad (5)$$

where σ_E, σ_I and n represent the standard deviation of potential noise, the standard deviation of current noise and total number of measurements, respectively. The noise resistance can be calculated from equation 6 [36]. Variation of R_n versus inhibitor concentration is shown in Figure 8.

$$R_n = \sigma_V / \sigma_I \quad (6)$$

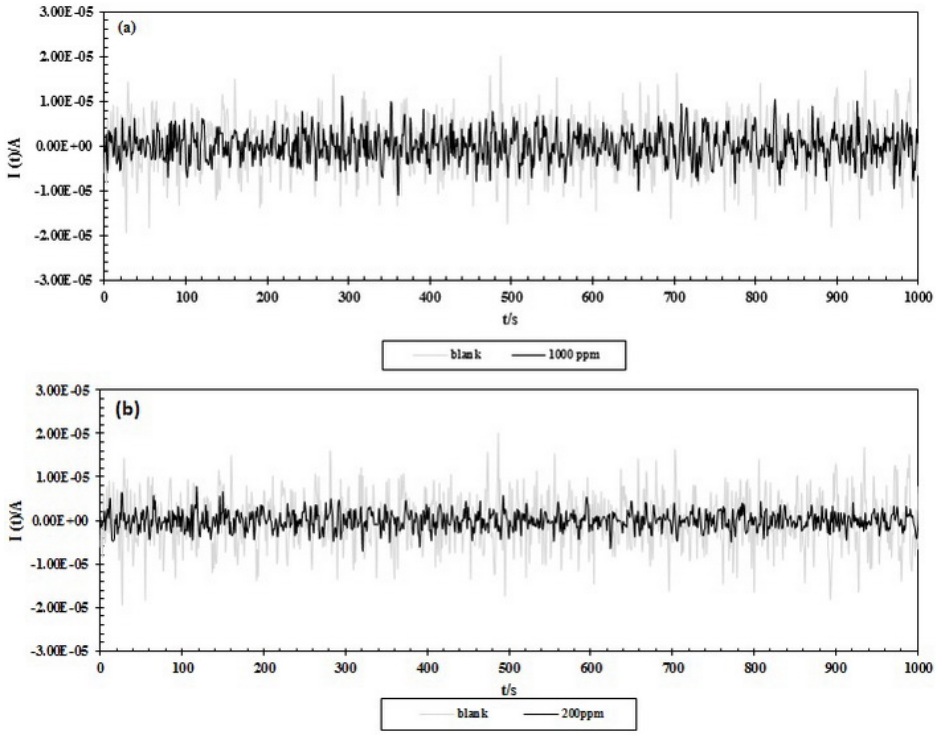

Figure 6. Current noise transients associated with Al samples exposed to 0.25 M HCl solution a) containing 0 and 1000 ppm BTH b) containing 0 and 200 ppm BT.

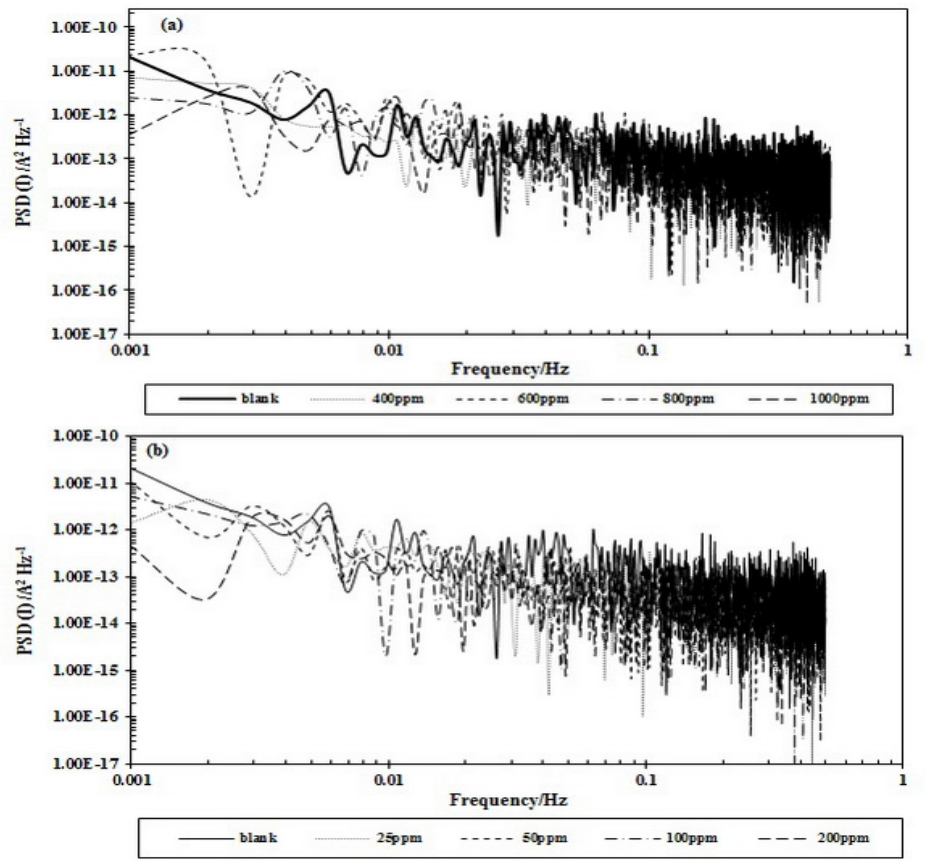

Figure 7. *PSD* (*I*) plots associated with Al samples exposed to 0.25 M HCl solution containing a) 0 to 1000 ppm BTH and b) 0 to 200 ppm BT.

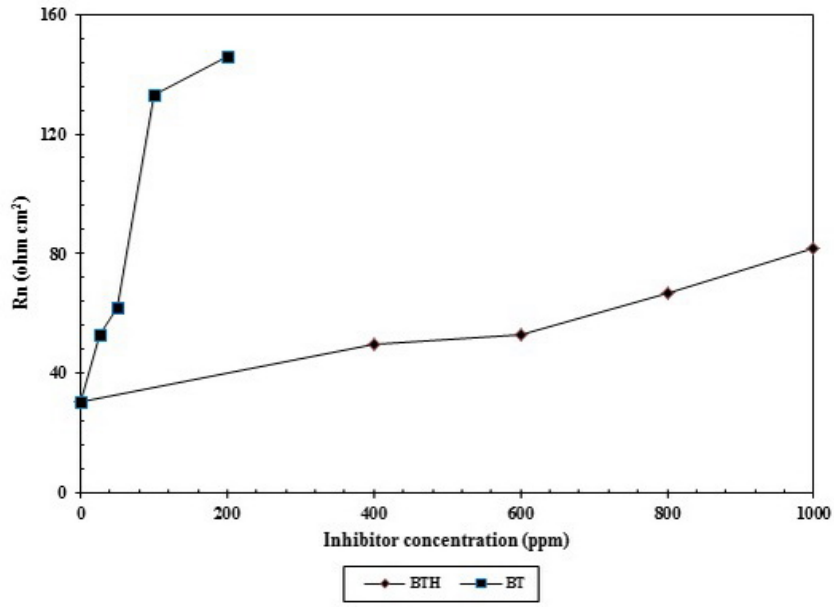

Figure 8. Variation of noise resistance (R_n) versus inhibitor concentration.

As can be seen in Figure 8, the R_n was increased in the presence of both inhibitors. The increase in R_n was more pronounced at higher inhibitors concentrations. It can be obviously seen that the increase in R_n was more and more pronounced in the case of using BT. This observation reveals the higher corrosion inhibition efficiency of BT compared with BTH. Also, these results are completely in agreement with the results obtained from the EIS and polarization measurements.

The shot noise theory [37] was employed to analyze EN data by considering current noise signals as packets of charge (q). The characteristic charge can be calculated from equation 7.

$$q = \sqrt{\Psi}_E \sqrt{\Psi_I}/B \quad (7)$$

where ψ_E, ψ_I, and B are low frequency *PSD* value of potential, low frequency *PSD* value of current and the Stern-Grey coefficient (the average value about 0.026 V), respectively.

It should be noted that in the case of aluminium alloy, the corrosion is likely to be localized and this may limit the applicability of the Stern-Geary coefficient. However, the localized corrosion is not that much significant for the aluminium alloy used in this study. Therefore, the Stern-Grey coefficient is applicable.

The characteristic charge (q) can provide useful information on mass loss during corrosion process in the presence and absence of BTH and BT [34, 35]. Variation of characteristic charge (q) versus inhibitor concentration is studied in Figure 9.

As can be seen in Figure 9, the characteristic charge (q) was reduced in the presence of both inhibitors. It can be obviously seen that the decrease in q was more and more pronounced at higher inhibitors concentrations. Results show that BT reduced characteristic charge (q) much greater than BTH. This observation reveals that the inhibitors could reduce oxidation rate of aluminum in HCl solution. This can be responsible for the q reduction on the surface of aluminum. The adsorption of inhibitors molecules on the surface of aluminum can be responsible for the characteristic charge reduction.

3.4. Scanning electron microscope (SEM) studies

SEM was utilized in order to investigate the aluminum surface morphology changes in the HCl solution in the presence and absence of the inhibitors. The SEM micrographs are shown in Figure 10.

Figure 10b shows a rough surface with corrosion products of aluminum after exposure to the HCl solution in the absence of inhibitors. This observation

reveals that HCl solution destroyed the aluminum surface significantly in the absence of inhibitors. However, addition of inhibitors to the HCl solution changed the visual performance of the surface of aluminum considerably. Figures 10c and 10d show that dissolution rate of aluminum was considerably reduced in the presence of both BT and BTH inhibitors. It can be seen that inhibitors have formed a protective film on the metal surface. However, the surface of sample exposed to HCl solution containing BT is smoother than the one containing BTH. Moreover, BT formed better passive film on the surface of aluminum. These results could support higher inhibition efficiency of BT compared with BTH.

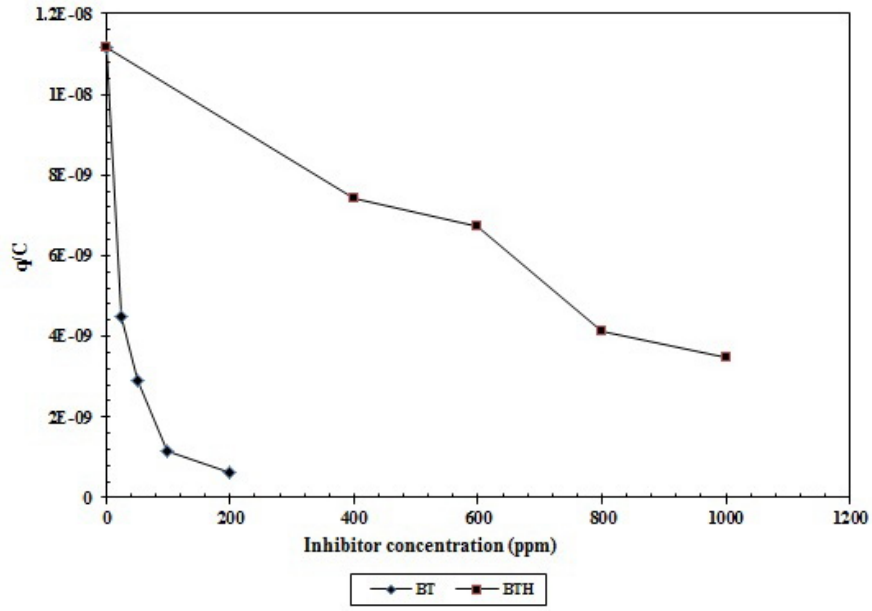

Figure 9. Variation of characteristic charge (*q*) versus inhibitor concentration.

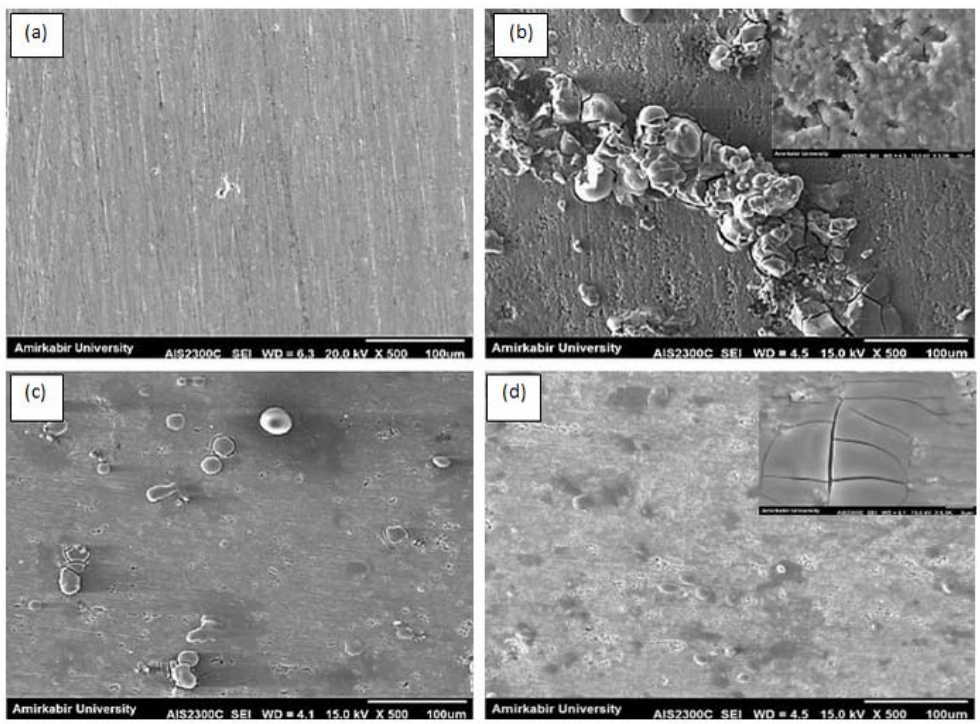

Figure 10. SEM micrographs of (a) blank Al sample before exposure to 0.25 M HCl (b) Al sample exposed to 0.25 M HCl, (c) Al sample exposed to 0.25 M HCl containing 1000 ppm BTH and (d) 200 ppm BT.

3.5. Corrosion inhibition efficiency evaluation

Results obtained from DC polarization, EIS and EN showed that the corrosion resistance of aluminum was enhanced in the presence of inhibitors in HCl solution. There was a good agreement between the results of various techniques. The corrosion inhibition efficiency values were calculated according to equations 8 to 10

$$EF\% = (1 - I/I_0) \times 100 \quad (8)$$

where EF%, I_0 and I represent corrosion inhibition efficiency, corrosion current density in the absence of the inhibitors, and corrosion current density in the presence of corrosion inhibitors, respectively.

$$EF\% = (R_{ct} - R_{ct}^{\circ})/R_{ct} \times 100 \quad (9)$$

where R_{ct} and R_{ct}^{0} show charge transfer resistance in the presence and absence of the inhibitors, respectively.

$$EF\,(ECN)\% = (R_n^{\circ} - R_n)/(R_n^{\circ}) \times 100 \quad (10)$$

where R_n and Rn^{0} represent noise resistance of the inhibited and uninhibited specimens, respectively. Variations of EF (%), calculated in DC, EIS and EN measurements, versus inhibitor concentration are shown in Figure 11.

As can be seen in Figure 11, the increase of inhibitors concentrations resulted in the increase in corrosion resistance of aluminum in 0.25 M HCl solution. The corrosion inhibition values > 0.6% and > 0.7% were obtained for the BTH and BT inhibitors, respectively. The same results were obtained in DC, EIS and EN measurements. It can be clearly seen that the corrosion inhibition values obtained in EN measurement (for BT) are higher than those obtained in DC and EIS measurements. However, the same trend can be seen for all the measurements. Two main reasons may be responsible for the higher corrosion inhibition efficiency obtained from EN compared with EIS and DC polarization. First, the experimental duration for the polarization measurement (which was about 10 min) was lower than the impedance study and EN (which were about 13 and 17 min, respectively). The higher experimental duration of the EN compared to DC polarization and EIS may increase the adsorption of inhibitor molecules on the metal surface [36].

As a result, the corrosion inhibition efficiency obtained from EIS and polarization measurements were lower than EN. The second reason is that noise resistance values obtained from EN are higher than polarization resistance values obtained from DC polarization and EIS. This may be attributed to the differences between the techniques for the evaluation of corrosion resistance of the metal in HCl solution. Other researchers also showed the same findings that noise resistance is greater than polarization resistances obtained from EIS and DC measurements [39].

It seems that the results obtained from the noise measurements are more accurate and reliable compared with EIS and DC polarization. Unlike EIS and DC polarization techniques, no external perturbation was applied to the samples during the measurements. Electrochemical noise data can be obtained from the appearance of fluctuations, statistical analysis and also shot noise theory. This means that EN data is more accurate than other electrochemical techniques.

3.6. Adsorption isotherm and inhibition mechanism of the inhibitors

The BTH and BT molecules have high tendency to be adsorbed on the surface of aluminum. The adsorption of inhibitor molecules on the metal surface occurs through water molecules replacement with organic inhibitors molecules. The mechanism is shown by equations 11 and 12 [40].

$$BTH_{sol} + H_2O_{ads} \rightarrow BTH_{ads} + H_2O_{sol} \quad (11)$$

$$BT_{sol} + H_2O_{ads} \rightarrow BT_{ads} + H_2O_{sol} \quad (12)$$

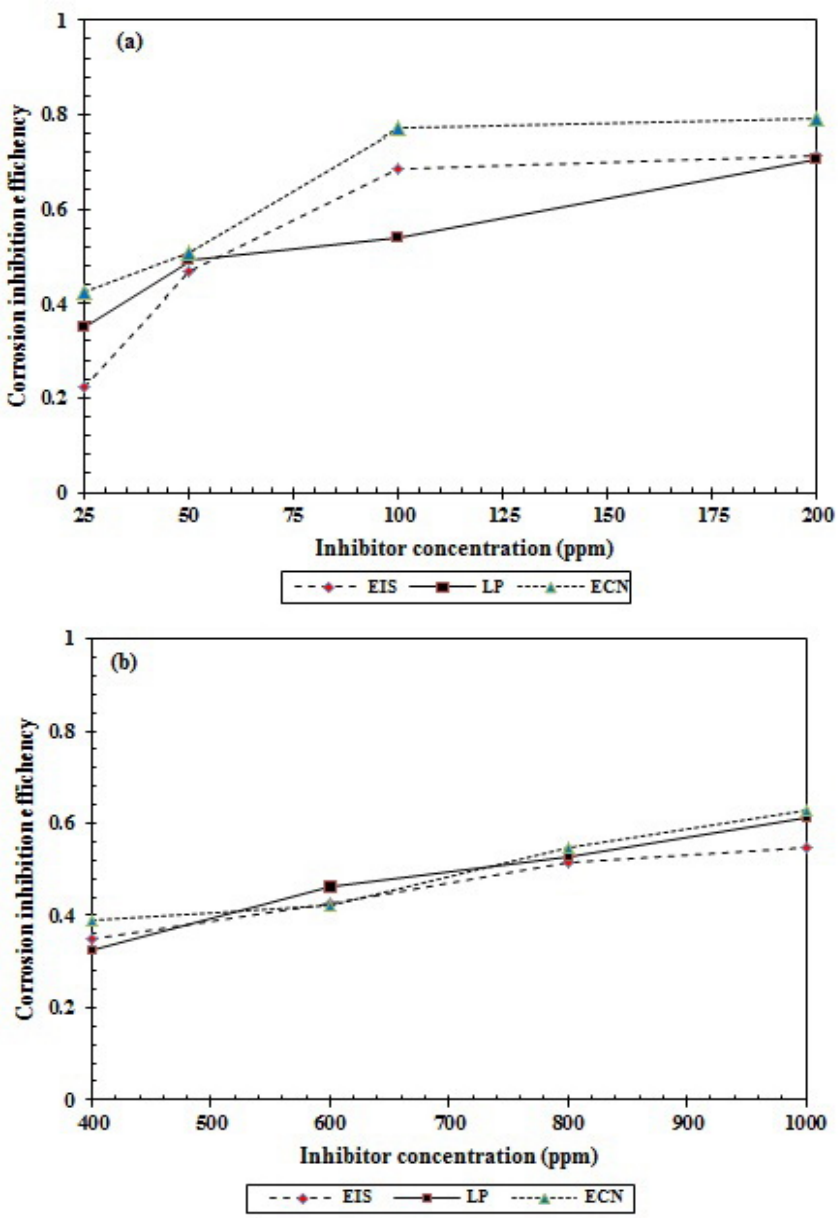

Figure 11. Variations of corrosion inhibition efficiency values of (a) BT and (b) BTH inhibitors versus inhibitors concentration.

Valuable information on the interaction of inhibitor and metal surface can be obtained by studying the mode of adsorption and adsorption isotherm. The experimental results were fitted to a series of adsorption isotherms including Langmuir [41], Frumkin [42], Temkin [43, 44] and Freundlich [45] (Figure 12). These isotherms are defined by equations 13 to 16.

$$\theta = 1/f \ \ln K(ads) + 1/f \ \ln C(ads) \quad \text{(Temkin isotherm)} \tag{13}$$

$$C(ads)/\theta = 1/(K(ads)) + C(ads) \quad \text{(Langmuir isotherm)} \tag{14}$$

$$\ln A/(C(ads)(1-\theta)) = \ln K + 2a\theta \quad \text{(Frumkin isotherm)} \tag{15}$$

$$\ln \theta = \log K + 1/(n \log C(ads)) \quad \text{(Freundlich isotherm)} \tag{16}$$

where θ, C(ads) and K(ads) are the degree of coverage on the metal surface, inhibitor concentration and the equilibrium constant for the adsorption-desorption process, respectively.

The correlation between K(ads) and ΔG^0(ads) is shown in equation 17:

$$\Delta G^\circ = RT \ln(55.5\,(K(ads)) \quad (17)$$

where R and T are the universal gas constant and the absolute temperature respectively. K(ads) and ΔG^0(ads) were obtained from EN, EIS and potentiodynamic measurements. Moreover, the regression coefficients were calculated from each isotherm and the results obtained are shown in Tables 4 and 5.

As can be seen in Tables 4 and 5, the regression coefficient values obtained from Langmuir adsorption isotherm are greater than the results obtained from other isotherms (Figure 12). This observation shows that the adsorption of BT and BTH molecules on the surface of aluminum obeys a Langmuir adsorption isotherm.

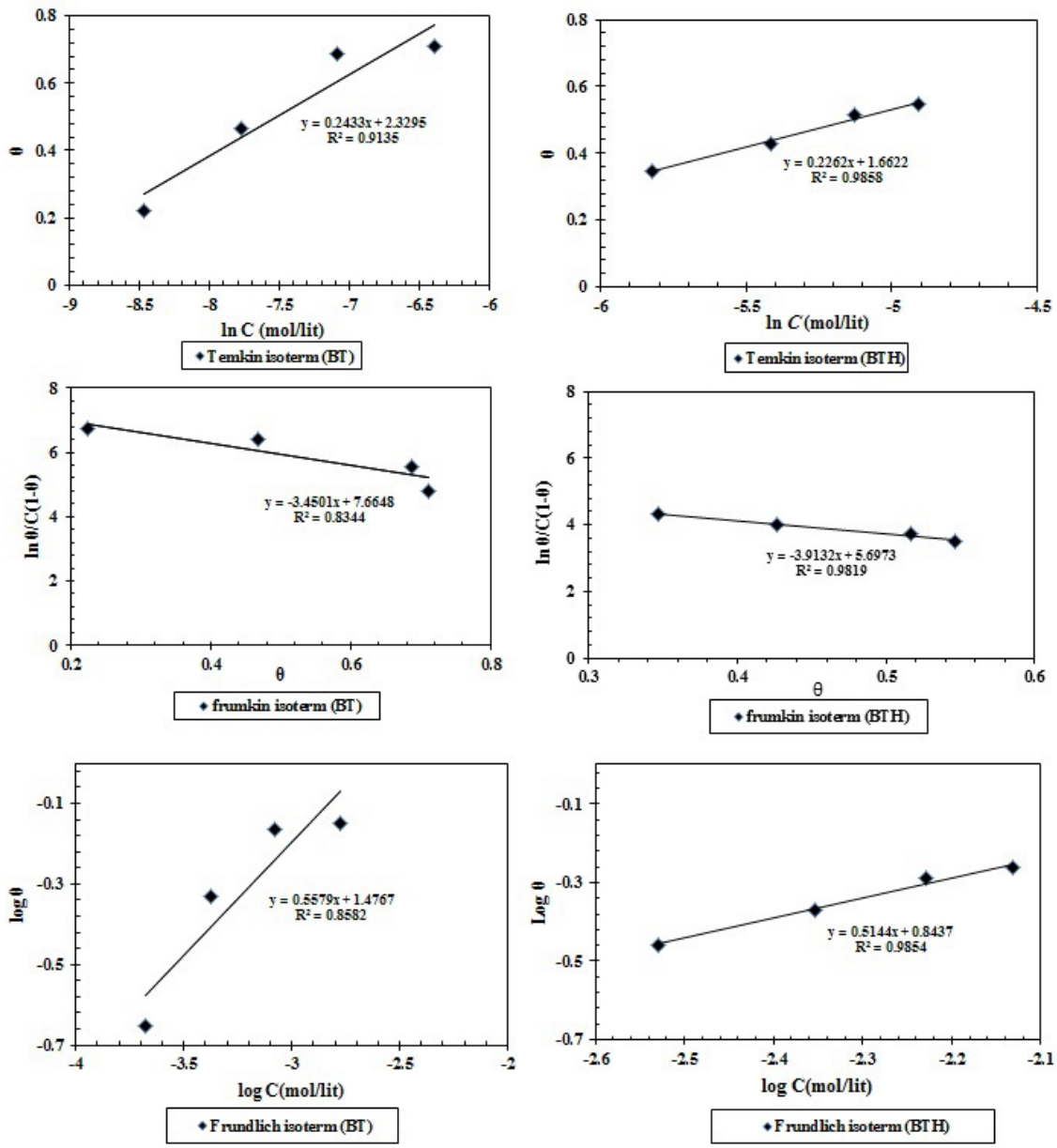

Figure 12. Different adsorption isotherms fitted on EIS results of Al samples exposed to 0.25 M HCl solution containing different concentrations of BTH and BT.

Table 4: The values of standard free energy of adsorption (ΔG^0(ads)) and regression coefficient (R^2) for the adsorption–desorption process obtained from different isotherms for BT and BTH inhibitors.

Sample	ΔG^0(ads) (kJ)			R^2		
	EIS	DC	EN	EIS	DC	EN
BT (Langmuir)	-28.0	-29.0	-29.7	0.94	0.98	0.98
BTH Langmuir)(	-22.7	-22.5	-22.1	0.98	0.85	0.96
BT (Frumkin)	-28.6	-32.5	-32.9	0.83	0.96	0.93
BTH (Frumkin)	-23.8	-22.8	-23.6	0.98	0.97	0.92
BT (Temkin)	-33.3	-36.0	-35.8	0.91	0.96	0.90
BTH (Temkin)	-27.8	-26.7	-27.4	0.98	0.99	0.90
BT (Freundlich)	-18.1	-13.9	-14.6	0.85	0.96	0.91
BTH (Freundlich)	-14.6	-16.7	-15.1	0.98	0.98	0.92

Table 5: The values of equilibrium constant (K(ads)) and regression coefficient (R^2) for adsorption–desorption process obtained from different adsorption isotherms for BT and BTH inhibitors.

Sample	K(ads) (M^{-1})			R^2		
	EIS	DC	EN	EIS	DC	EN
BT (Langmuir)	1.6×10^3	2.5×10^3	3.3×10^3	0.94	0.98	0.98
BTH (Langmuir)	1.8×10^3	1.7×10^3	1.4×10^3	0.98	0.8	0.96
BT (Frumkin)	2.1×10^3	1.0×10^4	1.2×10^4	0.83	0.96	0.93
BTH (Frumkin)	2.9×10^2	2.0×10^2	2.7×10^2	0.98	0.97	0.92
BT (Temkin)	1.4×10^4	4.3×10^4	4.0×10^4	0.91	0.96	0.90
BTH (Temkin)	1.5×10^3	9.9×10^2	1.3×10^3	0.98	0.99	0.90
BT (Freundlich)	29.9	5.3	6.9	0.85	0.96	0.91
BTH (Freundlich)	6.9	16.9	8.5	0.98	0.98	0.92

Table 4 shows the higher free energy of adsorption for the BT compared with BTH. This observation reveals the higher adsorption of BT molecules on the surface of metal compared with BTH. The negative values of ΔG^0(ads) show the spontaneous adsorption of BTH and BT molecules on the surface of aluminum. Table 5 shows higher *K*(ads) for the BT compared with BTH. These results indicate that BT is a better inhibitor for the aluminum protection against corrosion in HCl solution compared with BTH. The BTH and BT inhibitors include heteroatoms (N and S). Therefore, the coordination between BTH and BT molecules and the surface of aluminum can occur via N and S atoms. The BTH and BT molecules can be oriented parallel or vertical to the metal surface. Stronger bonds between inhibitors molecules and aluminum surface can be formed when the orientation of the inhibitor molecule is parallel to the aluminum surface. This can be attributed to the interaction of p electrons of the ring with vacant d orbitals of aluminum. In this way, the inhibitors molecules tend to be adsorbed by the aluminum surface and form complex film on the metal surface.

It has been shown that ΔG^0(ads)= -20 kJ mol^{-1} or ΔG^0(ads)< -20 kJ mol^{-1} are associated with an electrostatic interaction between charged molecules and charged metal surface (physical adsorption) [43-44]. On the other hand, ΔG^0(ads)=-40 kJ mol^{-1} or ΔG^0(ads)>-40 kJ mol^{-1} are associated with charge

sharing or transfer from the inhibitor molecules to the metal surface to form a co-ordinate covalent bond (chemical adsorption) [46, 47].The values of standard free energy of adsorption between -40 kJ mol^{-1} $<\Delta G^0(ads)<$-20 kJ mol^{-1} show mixed type adsorption (both chemical and physical interactions). Based on these explanations and the results shown in Tables 4 and 5, it can be found that the adsorption of BTH and BT molecules on the surface of aluminum occurred through both chemical and physical interactions. However, $\Delta G^0(ads)$ values of BTH are more close to -20 kJ mol^{-1}. Therefore, the adsorption of BTH on the surface of aluminum is predominantly physisorption. On the other hand, $\Delta G^0(ads)$ values of BT are close to -30 kJ mol^{-1} indicating more chemical interactions between this inhibitor and metal surface compared with BTH. BT includes 3 N atoms but BTH consists of one N and one S atom. The higher number of nitrogen atoms of BT than BTH can be responsible for the greater ability of this inhibitor to produce stronger physical/chemical bonds with the metal surface.

4. Conclusions

The corrosion inhibition properties of BTH and BT on aluminum in 0.25 M HCl solution were studied. The corrosion protection properties of the inhibitors were studied by analytical techniques including EIS, EN and DC polarization. Results showed good corrosion inhibition effects of BTH and BT on aluminum in 0.25 M HCl solution. The corrosion current density of aluminum in 0.25 M HCl was significantly increased in the presence of both inhibitors. Results showed higher corrosion inhibition properties of BT compared with BTH. The EN measurements revealed that both inhibitors increased noise resistance (R_n) and reduced characteristic charge (q) significantly. The increase in R_n and the decrease in characteristic charge (q) were more pronounced in the presence of BT compared with BTH. It was found that the best fit to the experimental data was Langmuir adsorption isotherm. The adsorption of both inhibitors on the surface of aluminum was based on physical and chemical adsorption (covalent bond). The high values of K(ads) and negative values of ΔG(ads) suggested that BT and BTH molecules highly tended to be adsorbed on the surface of aluminum. The greater K(ads) and more negative ΔG(ads) values of BT compared with BTH were observed.

5. References

1. G. E. Totten, Handbook of aluminium: Physical metallurgy and processes, Vol.1, Marcel Dekker, Inc., ISBN 0-8247-0494-0 (2003).
2. C. Varg, Corrosion of aluminum. Elsevier Ltd (2004).
3. H. P. Godard, W. P. Jepson, M. R. Bothwell, R.L. Kane, The Corrosion of Light Metals, first ed John Wiley & Sons, New York (1967).
4. O. K. Abiola and J. O. E. Otaigbe, Effect of common water contaminants on the corrosion of aluminium alloys in ethylene glycol–water solution, *Corros. Sci.,* 50(2010), 242-247.
5. F. Elshawesh, M. El Agaili, A. Elwaer, Demineralised water and corrosion, Br. *Corros. J.,* 32(1997), 77-83.
6. A. S. Elola, T. F. Otero, A. Porro, Evolution of the Pitting of Aluminum Exposed to the Atmosphere, *Corrosion.,* 48(1992), 854-863
7. R. Vera, D. Delgado, B.M. Rosales, Effect of atmospheric pollutants on the corrosion of high power electrical conductors: Part 1. Aluminium and AA6201 alloy, *Corros. Sci.,* 48(2006), 2882-2900.
8. Q. Le Thu, G. P. Bierwagen, S. Touzain, EIS and ENM measurements for three different organic coatings on aluminum, *Prog. Org. Coat.,* 42(2001), 179-187.
9. Y. J. Du, M. Damron, G. Tang, H. Zheng, C. J. Chu, J. H. Osborne, Inorganic/organic hybrid coatings for aircraft aluminum alloy substrates, *Prog. Org. Coat.,* 41(2001), 226-232.
10. M. Bethencourt, F. J. Botana, J. J. Calvino, M. Marcos, M. A. RodrÍguez-Chacón, Lanthanide compounds as environmentally-friendly corrosion inhibitors of aluminium alloys: a review, *Corros. Sci.,* 40(1998), 1803-1819.
11. I. B. Obot, N. O. Obi-Egbedi, S. A. Umoren, I. B. Obot, N. O. Obi-Egbedi, S. A. Umoren, Antifungal drugs as corrosion inhibitors for aluminium in 0.1 M HCl, *Corros. Sci.,*

51(2009), 1868-1875.

12. O. K. Abiola, J. O. E. Otaigbe, O. J. Kio, Gossipium hirsutum L. extracts as green corrosion inhibitor for aluminum in NaOH solution', *Corros. Sci.,* 51(2009), 1879-1881.
13. B. V. Appa Rao, K. Chaitanya Kumar, Effect of Hydrodynamic Conditions on Corrosion Inhibition of CueNi (90/10) Alloy in Seawater and Sulphide Containing Seawater Using 1,2,3-Benzotriazole, *J. Mater. Sci. Technol.,* 30(2014), 65-76.
14. B. Müller, S. Fischer, Epoxy ester resins as corrosion inhibitors for aluminium and zinc pigments, *Corros. Sci.,* 48(2006), 2406-2416.
15. A. Ghanbari, M. M. Attar, M. Mahdavian, Acetylacetonate Complexes as New Corrosion Inhibitors in Phosphoric Acid Media: Inhibition and Synergism Study, Prog. Color Colorants Coat., 2 (2009), 115-122.
16. E. Alibakhshi, E. Ghasemi, M. Mahdavian, A Comparison Study on Corrosion Behavior of Zinc Phosphate and Potassium Zinc Phosphate Anticorrosive Pigments, Prog. Color Colorants Coat., 5(2012), 91-99.
17. A. Ghanbari, M. M. Attar, Mild Steel Surface Pretreatment Using Phosphoric acid-Inhibitor Solution, Prog. Color Colorants Coat., 7(2014), 269-284.
18. L. L. Shreir, R. A. Jarman, G. T. Burstein, corrosion volume 1, Metal Environment Reactions, Butterworth-Heinemann (2000)
19. S. A. Ali, H. A. Al-Muallem, S. U. Rahman, M. T. Saeed, Bis-isoxazolidines: A new class of corrosion inhibitors of mild steel in acidic media, *Corros. Sci.,* 50 (2008), 3070-3077.
20. E. Samiento-Bustos, J. G. González Rodriguez, J. Uruchurtu, G. Dominguez-Patiño, V. M. Salinas-Bravo, Effect of inorganic inhibitors on the corrosion behavior of 1018 carbon steel in the LiBr + ethylene glycol + H2O mixture, *Corros. Sci.,* 50(2008), 2296-2303.
21. D. Zhang, Z. An, Q. Pan, L. Gao, G. Zhou, Comparative study of bis-piperidiniummethyl-urea and mono-piperidiniummethyl-urea as volatile corrosion inhibitors for mild steel, *Corros. Sci.*, 48(2006), 1437-1448.
22. G. Gao, C. H. Liang, 1,3-Bis-diethylamino-propan-2-ol as volatile corrosion inhibitor for brass, *Corros. Sci.,* 49(2007), 3479-3493.
23. H. Ashassi-Sorkhabi, B. Shabani, B. Aligholipour, D. Seifzadeh, The effect of some Schiff bases on the corrosion of aluminum in hydrochloric acid solution, *Appl. Surf. Sci.,* 252 (2006), 4039-4047.
24. M. Abdallah, Antibacterial drugs as corrosion inhibitors for corrosion of aluminium in hydrochloric solution, *Corros. Sci.,* 46(2004), 1981-1996.
25. S. Safak, B. Duran, A. Yurt, G. Turkoglu, Schiff bases as corrosion inhibitor for aluminium in HCl solution, *Corros. Sci.,* 54(2012), 251-259.
26. M. M. Fares, A. K. Maayta, M. M. Al-Qudah, Pectin as promising green corrosion inhibitor of aluminum in hydrochloric acid solution, *Corros. Sci.,* 60(2012), 112-117.
27. N. Kovacevic, A. Kokalj, The relation between adsorption bonding and corrosion ... and metal surfaces, *Mater. Chem. Phys.,* 137(2012), 331-339.
28. B. P. Markhali, R. Naderi, M. Mahdavian, M. Sayebani, S.Y. Arman, Electrochemical impedance spectroscopy and electrochemical noise measurements as tools to evaluate corrosion inhibition of azole compounds on stainless steel in acidic media, *Corros Sci.,* 75 (2013), 269-279.
29. J. R. Kearns, J. R. Scully, P. R. Roberge, D. L. Reichert, J. L. Dawson (Eds) ASTM Int'l (1996).
30. Y. L. Cheng, Z. Zhang, F. H. Cao, J. F. Li, J. Q. Zhang, J. M. Wang, C. N. Cao, *Mater Corros.,* 54(2003), 601-608.
31. S. Deng, X. Li, Inhibition by Jasminum nudiflorum Lindl. leaves extract of the corrosion of aluminium in HCl solution, *Corros Sci.,* 64(2012), 253-262.
32. X. Li, S. Deng, H. Fu, Inhibition by tetradecylpyridinium bromide of the corrosion of aluminium in hydrochloric acid solution, *Corros Sci.,* 53(2011), 1529-1536.
33. K. F. Khaled, M. M. Al-Qahtani, The inhibitive effect of some tetrazole derivatives towards Al corrosion in acid solution: Chemical, electrochemical and theoretical studies, *Mater Chem Phys.,* 113(2009), 150-158.
34. A. Yurt, S. Ulutas, H. Dal, Electrochemical and theoretical investigation on the corrosion of aluminium in acidic solution containing some

Schiff bases, *Appl Surf Sci.,* 253(2006), 919-925.
35. Q. B. Zhang, Y. X. Hua, Corrosion inhibition of aluminum in hydrochloric acid solution by alkylimidazolium ionic liquids, *Mater Chem Phys.*, 119(2010), 57-64.
36. C. Valentini, J. Fiora, G. Ybarra, A comparison between electrochemical noise and electrochemical impedance measurements performed on a coal tar epoxy coated steel in 3% NaCl*, Prog Org Coat.,* 73(2012), 173-177.
37. J. M. Sanchez-Amaya, R. A. Cottis, F. J. Botana, Shot noise and statistical parameters for the estimation of corrosion mechanisms*, Corros Sci.,* 47(2005), 3280-3299.
38. R. Naderi, M. M. Attar, Application of the electrochemical noise method to evaluate the effectiveness of modification of zinc phosphate anticorrosion pigment, *Corros Sci.,* 51(2009), 1671-1674.
39. P. Bothi Raja, A. Kaleem Qureshi, A. Abdul Rahim, H. Osman, K. Awang, Neolamarckia cadamba alkaloids as eco-friendly corrosion inhibitors for mild steel in 1 M HCl media, *Corros Sci.,* 69(2013), 292-301.
40. A. Döner, R. Solmaz, M. Ozcan, G. Kardas, Experimental and theoretical studies of thiazoles as corrosion inhibitors for mild steel in sulphuric acid solution, *Corros Sci.,* 53(2011), 2902-2932.
41. B. Jom, R. Akn, Modern Electrochemistry, Volume 2, Plenum Publishing Corporation, New York (1976).
42. X. Li, S. Deng, Inhibition effect of Dendrocalamus brandisii leaves extract on aluminum in HCl, H3PO4 solutions, *Corros Sci.*, 65(2012), 299-308.
43. E. Geler, D. S. Azambuja, Corrosion inhibition of copper in chloride solutions by pyrazole, *Corros Sci.,* 42(2000), 631-643.
44. D. Seifzadeh, H. Basharnavaz, A. Bezaatpour, A Schiff base compound as effective corrosion inhibitor for magnesium in acidic media, *Mater Chem Phys.,* 138(2013), 794-802.
45. N. O. Obi-Egbedi, I. B. Obot, Inhibitive properties, thermodynamic and quantum chemical studies of alloxazine on mild steel corrosion in H_2SO_4, *Corros Sci.,* 53(2011), 263-275.
46. X. Wang, H. Yang, F. Wang, An investigation of benzimidazole derivative as corrosion inhibitor for mild steel in different concentration HCl solutionsm, *Corros Sci.,* 53(2011), 113-121.
47. N. A. Negm, Y. M. Elkholy, M. K. Zahran, S. M. Tawfik, Corrosion inhibition efficiency and surface activity of benzothiazol-3-ium cationic Schiff base derivatives in hydrochloric acid, *Corros Sci*., 52(2010), 3523-3536.